

# Heavy target fragment yields in the interaction of 28 GeV protons with $^{238}\text{U}$

B. V. JACAK,<sup>1</sup> W. LOVELAND,<sup>2</sup> D. J. MORRISSEY,<sup>1</sup> P. L. MCGAUGHEY, and G. T. SEABORG  
*Nuclear Science Division, Lawrence Berkeley Laboratory, University of California, Berkeley, CA 94720, U.S.A.*

Received August 31, 1982

*This paper is dedicated to Professor Leo Yaffe on the occasion of his 65th birthday*

B. V. JACAK, W. LOVELAND, D. J. MORRISSEY, P. L. MCGAUGHEY, and G. T. SEABORG. *Can. J. Chem.* **61**, 701 (1983).

The yields of target fragments from the interaction of 28 GeV protons with  $^{238}\text{U}$  have been measured, with special attention being given to those fragments with  $160 \leq A \leq 200$ . From the measured fragment yields, isobaric production cross sections were calculated. Significant yields ( $\sigma(A) \sim 1-10$  mb) of heavy target fragments ( $160 \leq A \leq 210$ ) were found. These fragments are believed to be the non-fissioning survivors from the population of highly excited residual nuclei produced in the initial p-nucleus collision. A pedagogical calculation of the fission - particle emission competition shows how the initial highly excited heavy nuclei could evaporate  $\sim 20-50$  particles while surviving fission competition.

B. V. JACAK, W. LOVELAND, D. J. MORRISSEY, P. L. MCGAUGHEY et G. T. SEABORG. *Can. J. Chem.* **61**, 701 (1983).

On a mesuré les rendements en fragments de cibles provenant de l'interaction de protons à 28 GeV avec  $^{238}\text{U}$ , en portant une attention spéciale aux fragments avec  $160 \leq A \leq 200$ . On a calculé les sections droites de production isobare à partir de la mesure de ces rendements de fragment. On a observé des rendements importants ( $\sigma(A) \sim 1-10$  mb) en fragments de cibles lourds ( $160 \leq A \leq 210$ ). On croit que ces fragments sont les survivants qui n'ont pas subi de fission et qui faisaient partie de la population de noyaux résiduels fortement excités produits lors de la collision initiale p-noyau. Un calcul pédagogique de la compétition entre l'émission des particules et la fission montre comment le noyau lourd fortement excité initialement peut disperser  $\sim 20-50$  particules tout en survivant à la compétition de fission.

[Traduit par le journal]

## Introduction

Five years ago, Loveland *et al.* (1) reported that in the interaction of 25 GeV  $^{12}\text{C}$  with  $^{238}\text{U}$ , one observed in addition to the expected fission fragments, large yields of heavy target fragments with  $160 \leq A \leq 200$ .<sup>3</sup> Subsequently, McGaughey *et al.* (2) reported observing the production of these fragments in the interaction of 8 GeV  $^{20}\text{Ne}$  with  $^{238}\text{U}$  although the magnitude of their yields was less. These observations were significant for a number of reasons. First, since such products had not been observed in the interaction of relativistic protons with  $^{238}\text{U}$  (see ref. 3 for a summary of these data), it appeared that these reaction products were produced by a mechanism unique to nucleus-U collisions as compared to nucleon-U collisions. A study of these products might then offer the possibility of studying unique aspects of nucleus-nucleus collisions. Second, the question arose as to how such products could be formed. If they were spallation products, that meant that  $\sim 60$  A units were removed from the target during the initial reaction and the subsequent deexcitation of the target fragment. Naively one might have expected the heavy nucleus to fission rather than allow such an extended evaporation process to occur.

Because of the importance of the issues raised by the observation of large heavy fragment yields in relativistic nucleus-U collisions, we thought it to be prudent to carefully re-examine the pattern of target fragment yields in relativistic p-U collisions to see if any evidence could be found for heavy target fragment survivors of the primary projectile-target encounter.

Accordingly we report in this paper the observation of such fragments, produced in significant quantities, in the interaction of 28 GeV p with  $^{238}\text{U}$ . We use a pedagogical model of fission - particle emission competition to show how these heavy target fragments could be formed from the highly excited products of the initial p-U collision.

## Experimental

A natural uranium foil of thickness  $33.5 \text{ mg/cm}^2$  surrounded by mylar catcher foils of thickness  $35.5 \text{ mg/cm}^2$  was irradiated for 63 min in an external beam of 28 GeV protons from the Alternating Gradient Synchrotron at Brookhaven National Laboratory with an average particle intensity of  $7.8 \times 10^{13}$  protons/min. The intensity of the beam striking the target was determined by measuring the yields of  $^{22}\text{Na}$  and  $^{24}\text{Na}$  in a  $12.72 \text{ mg/cm}^2$  Al foil irradiated simultaneously with the U foil. The following monitor production cross sections (4) were used:  $\sigma(^{24}\text{Na}) = 8.0 \pm 0.3$  mb;  $\sigma(^{22}\text{Na}) = 9.8 \pm 1.0$  mb.

Following a one day delay for shipment of the irradiated foils to the Lawrence Berkeley Laboratory, analysis of the radioactivities of the target fragments began. The irradiated U foil and the mylar catcher foils were cut approximately in half; the target was counted before and after the cutting process, allowing an exact determination of the relative fractions. One half of the target and its associated mylar catcher foils were subjected to direct  $\gamma$ -ray spectroscopy, while a chemical group separation procedure was applied to the other  $33.5 \text{ mg/cm}^2$  U foil half without its catcher foils. In the former case, all of the target fragments should have been stopped in the U foil-catcher assembly (5-15); in the latter case, attention was focused on the yields of the heavy ( $160 \leq A \leq 210$ ) fragments and based upon prior experiments on the ranges of n-deficient heavy rare-earth nuclides (12), only a negligible fraction of the total yield of these products should escape from the U foil. (For the yields of the As and Sb isotopes measured by radiochemical techniques and direct foil counting, no discernible difference between the two measurement techniques was noted.) The chemical procedure used was that developed by Kratz and co-workers (16) with minor modifications. It is based on the volatility and ion exchange behavior of the bromide complexes of the elements. Chem-

<sup>1</sup>Present address: National Superconducting Cyclotron Laboratory, Michigan State University, East Lansing, MI 48824, U.S.A.

<sup>2</sup>Present address: Department of Chemistry, Oregon State University, Corvallis, OR 97331, U.S.A.

<sup>3</sup>The heavy fragment yields reported in ref. 1 are now known to be overestimates due to difficulties in integrating the charge dispersions to give isobaric yields.

TABLE 1. Target fragment yields in the interaction of 28 GeV p + <sup>238</sup>U

Nuclide	Measured production cross section (mb)	Previous results (mb)	Calculated independent yield (mb)	Isobaric yield (mb)	Nuclide	Measured production cross section (mb)	Previous results (mb)	Calculated independent yield (mb)	Isobaric yield (mb)
<sup>71</sup> As	3.4 ± 0.2	1.2 <sup>a</sup>	3.4 ± 0.3	19.3 ± 1.9	<sup>127</sup> Cs	7.7 ± 0.6		7.6 ± 0.8	8.7 ± 0.9 <sup>i</sup>
<sup>72</sup> As	4.7 ± 0.3 <sup>j</sup>	4 <sup>a</sup>	4.5 ± 0.5	18.4 ± 1.8	<sup>128</sup> Sb	2.7 ± 0.1 <sup>j</sup>		1.9 ± 0.2	20.8 ± 2.1 <sup>k</sup>
<sup>74</sup> As	6.9 ± 0.3 <sup>j</sup>	6.2 <sup>a</sup>	6.9 ± 0.7	18.2 ± 1.8	<sup>128</sup> Ba	2.6 ± 0.09	(6.5 ± 0.5 <sup>d</sup> )	2.6 ± 0.3	10.7 ± 1.1 <sup>i</sup>
<sup>76</sup> As	6.2 ± 0.4 <sup>j</sup>	8.0 ± 2.0 <sup>b</sup>	6.2 ± 0.6	22.0 ± 2.2	<sup>129</sup> Cs	8.3 ± 2.4	6.0 ± 0.3 <sup>k</sup>	1.8 ± 0.5	7.8 ± 2.3 <sup>i</sup>
<sup>84</sup> Rb	8.5 ± 0.05	6.9 ± 0.3 <sup>c</sup>	8.5 ± 0.8	21.4 ± 2.1	<sup>132</sup> La	13.1 ± 0.07	(9.5 ± 0.2 <sup>f</sup> )	10.8 ± 1.1	11.9 ± 1.2 <sup>k</sup>
<sup>86</sup> Y	3.7 ± 0.4		3.2 ± 0.3	24.8 ± 2.6	<sup>141</sup> Ce	6.2 ± 0.3		3.5 ± 0.3	14.1 ± 1.4 <sup>i</sup>
<sup>87</sup> Y	7.2 ± 0.08		6.1 ± 0.6	25.4 ± 2.5	<sup>143</sup> Ce	4.3 ± 0.2	6.8 ± 0.5 <sup>i</sup>	2.7 ± 0.3	15.2 ± 1.5 <sup>i</sup>
<sup>87M</sup> Y	9.0 ± 0.8		7.5 ± 0.7	31.3 ± 3.1	<sup>145</sup> Eu	4.7 ± 0.08	7.1 ± 0.9 <sup>h</sup>	1.8 ± 0.2	4.8 ± 0.5
<sup>88</sup> Zr	4.6 ± 0.2		4.2 ± 0.7	39.8 ± 4.0	<sup>147</sup> Gd	3.8 ± 2.2	4.0 ± 0.4 <sup>i</sup>	2.4 ± 1.4	3.9 ± 2.3
<sup>89</sup> Zr	4.4 ± 0.2		3.7 ± 0.4	18.1 ± 1.8	<sup>149</sup> Gd	5.0 ± 0.7	5.9 ± 0.8 <sup>h</sup>	0.94 ± 0.12	5.4 ± 0.7
<sup>90</sup> Nb	2.7 ± 0.2		2.4 ± 0.2	28.8 ± 2.9	<sup>151</sup> Tb	8.9 ± 5.7	3.1 ± 0.3 <sup>i</sup>	3.5 ± 2.3	9.0 ± 5.8
<sup>91</sup> Sr	8.7 ± 0.5	(14.3 ± 0.4 <sup>d</sup> )			<sup>152</sup> Tb	3.1 ± 0.04	4.7 ± 0.5 <sup>h</sup>	0.54 ± 0.05	3.0 ± 0.3
<sup>92M</sup> Nb	0.24 ± 0.08		0.24 ± 0.08	14.2 ± 1.4	<sup>160</sup> Er	2.7 ± 0.8	6.5 ± 1.0 <sup>h</sup>	2.7 ± 0.8	2.7 ± 0.8
<sup>93M</sup> Mo	0.82 ± 0.34		0.82 ± 0.34	20.9 ± 2.1	<sup>166</sup> Yb	6.2 ± 0.3	4.5 ± 0.5 <sup>i</sup>	6.2 ± 0.6	6.9 ± 0.7
<sup>95</sup> Zr	13.5 ± 0.4		12.8 ± 1.3	23.9 ± 2.4	<sup>171</sup> Lu	3.2 ± 0.1	4.9 ± 0.5 <sup>h</sup>	1.1 ± 0.1	3.7 ± 0.4
<sup>95</sup> Nb	7.7 ± 0.8		7.7 ± 0.8	20.9 ± 2.1	<sup>173</sup> Hf	5.2 ± 0.4	0.034 ± 0.041 <sup>h</sup>	2.6 ± 0.3	5.1 ± 0.5
<sup>95</sup> Tc	3.2 ± 0.07		2.9 ± 0.3	9.7 ± 1.0	<sup>182</sup> Os	4.1 ± 0.3		4.0 ± 0.4	13.2 ± 1.3
<sup>96</sup> Nb	5.4 ± 0.5		5.4 ± 0.5	83.9 ± 8.4	<sup>185</sup> Ir	2.9 ± 0.5 <sup>j</sup>		2.8 ± 0.5	9.4 ± 1.7
<sup>96</sup> Tc	2.18 ± 0.06		2.2 ± 0.2	—	<sup>186</sup> Ir	2.4 ± 0.9 <sup>j</sup>		2.3 ± 0.9	4.3 ± 1.6
<sup>97</sup> Zr	11.8 ± 1.2		11.8 ± 1.2	—	<sup>188</sup> Ir	6.6 ± 2.2 <sup>j</sup>		4.6 ± 1.6	7.2 ± 2.5
<sup>99</sup> Mo	17.0 ± 0.4		11.5 ± 1.1	32.9 ± 3.3	<sup>190</sup> Ir	1.1 ± 0.1 <sup>j</sup>		1.1 ± 0.1	5.4 ± 0.6
<sup>100</sup> Rh	2.3 ± 0.5		2.2 ± 0.5	43.6 ± 9.2	<sup>191</sup> Pt	10.3 ± 1.9		7.0 ± 1.3	11.0 ± 2.1
<sup>101M</sup> Rh	4.0 ± 0.5		4.0 ± 0.5	—	<sup>192</sup> Ir	0.18 ± 0.07 <sup>j</sup>		0.18 ± 0.07	10.5 ± 3.9
<sup>105</sup> Ru	10.4 ± 0.2		8.3 ± 0.8	37.3 ± 3.7	<sup>195M</sup> Hg	1.2 ± 0.2		1.2 ± 0.2	—
<sup>105</sup> Rh	20.7 ± 1.4		12.3 ± 1.2	32.2 ± 3.2	<sup>201</sup> Pb	2.6 ± 0.2		2.6 ± 0.3	3.4 ± 0.3
<sup>106M</sup> Ag	2.1 ± 0.2		2.1 ± 0.2	—	<sup>203</sup> Pb	3.1 ± 0.2		1.9 ± 0.2	2.9 ± 0.3
<sup>111</sup> In	5.0 ± 0.1	5.0 ± 0.5 <sup>c</sup>	4.2 ± 0.4	22.9 ± 2.3	<sup>203</sup> Bi	0.71 ± 0.37 <sup>j</sup>		0.71 ± 0.37	2.0 ± 1.1
<sup>118M</sup> Sb	2.0 ± 0.1 <sup>j</sup>		2.0 ± 0.2	—	<sup>204</sup> Bi	2.9 ± 0.4 <sup>j</sup>		2.9 ± 0.4	3.8 ± 0.5
<sup>119M</sup> Te	2.1 ± 0.7 <sup>j</sup>		2.1 ± 0.7	—	<sup>205</sup> Bi	3.5 ± 0.4 <sup>j</sup>		3.3 ± 0.4	3.7 ± 0.4
<sup>120</sup> Sb	3.4 ± 0.1 <sup>j</sup>		3.4 ± 0.3	—	<sup>207</sup> Po	3.0 ± 0.5		2.9 ± 0.5	3.9 ± 0.7
<sup>121</sup> Te	4.4 ± 0.4		3.4 ± 0.3	4.4 ± 0.4 <sup>k</sup>	<sup>232</sup> Pa	3.6 ± 0.3		3.6 ± 0.4	5.2 ± 0.5
<sup>122</sup> Sb	5.7 ± 0.3 <sup>j</sup>		5.6 ± 0.6	22.0 ± 2.2 <sup>i</sup>	<sup>233</sup> Pa	9.8 ± 0.5		9.2 ± 0.9	10.2 ± 1.0
<sup>123</sup> I	6.9 ± 0.04	(9.5 ± 0.3 <sup>f</sup> )	6.0 ± 0.6	6.9 ± 0.7 <sup>k</sup>	<sup>234</sup> Pa	3.2 ± 0.9		3.2 ± 0.9	4.3 ± 1.2
<sup>124</sup> Sb	5.6 ± 0.3 <sup>j</sup>		5.6 ± 0.6	23.1 ± 2.3 <sup>i</sup>					
<sup>124</sup> I	2.2 ± 0.1	(3.0 ± 0.1 <sup>f</sup> )	2.2 ± 0.2	5.5 ± 0.5 <sup>k</sup>					
<sup>125</sup> Xe	6.3 ± 2.3	6.4 ± 1 <sup>b</sup>	6.0 ± 2.2	6.6 ± 2.4 <sup>k</sup>					
<sup>126</sup> Sb	3.7 ± 0.2 <sup>j</sup>		3.7 ± 0.4	21.7 ± 2.2 <sup>k</sup>					
<sup>127</sup> Sb	7.2 ± 0.4 <sup>j</sup>		2.6 ± 0.3	19.8 ± 2.0 <sup>k</sup>					

<sup>a</sup>Reference 35.

<sup>b</sup>Reference 36.

<sup>c</sup>Reference 37.

<sup>d</sup>Reference 38 (11.5 GeV p).

<sup>e</sup>Reference 39.

<sup>f</sup>Reference 40 (11.5 GeV p).

<sup>g</sup>Reference 41.

<sup>h</sup>Reference 3.

<sup>i</sup>Reference 42.

<sup>j</sup>Yields from chemically separated fraction.

<sup>k</sup>Isobaric yield from n-poor portion of charge distribution.

<sup>l</sup>Isobaric yield from n-rich portion of charge distribution.

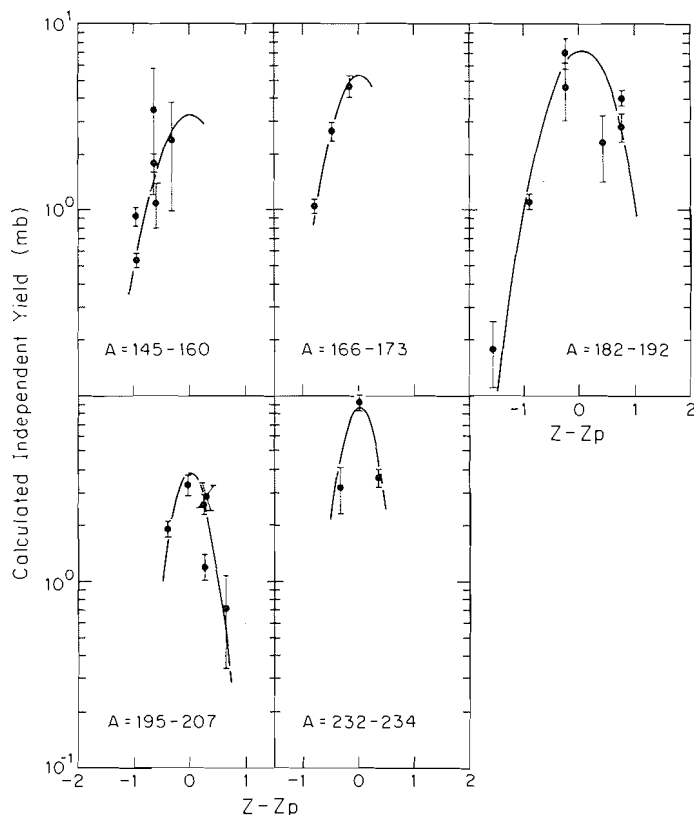


FIG. 1. The charge dispersion curves obtained in this work for the heaviest target fragments are shown as a function of the mass region of the products. The parameters that describe the center and width of the individual curves are given in Table 2.

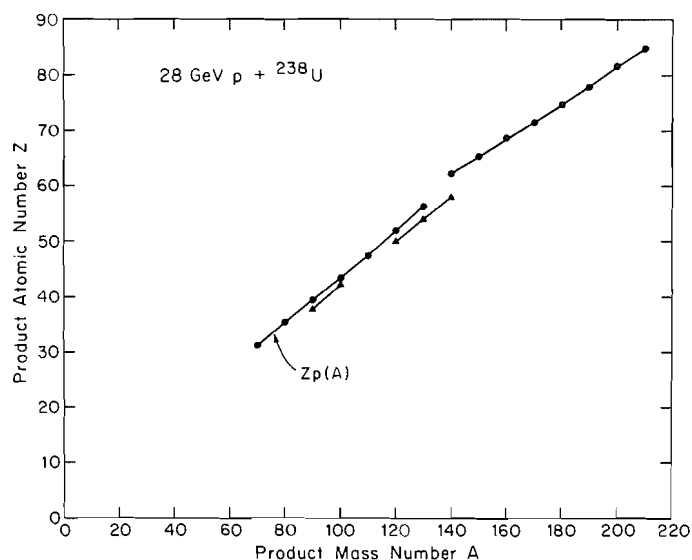


FIG. 2. The values of the most probable primary fragment charge,  $Z_p$ , as determined by fitting the data in Figs. 1 and 3 are shown as a function of product mass number. For  $84 \leq A \leq 96$  and  $118 \leq A \leq 143$ , the  $Z_p$  corresponding to both the n-rich and n-deficient components of the charge distribution are shown.

ical yields of various elements were calculated by comparison of the separated radioactivities with those in the unseparated foil or where available, by the yield of various tracers employed in the chemistry.

The assay of the target fragment radioactivities and the calculation of measured nuclidic production cross sections from them was done using standard techniques that have been described previously (17).

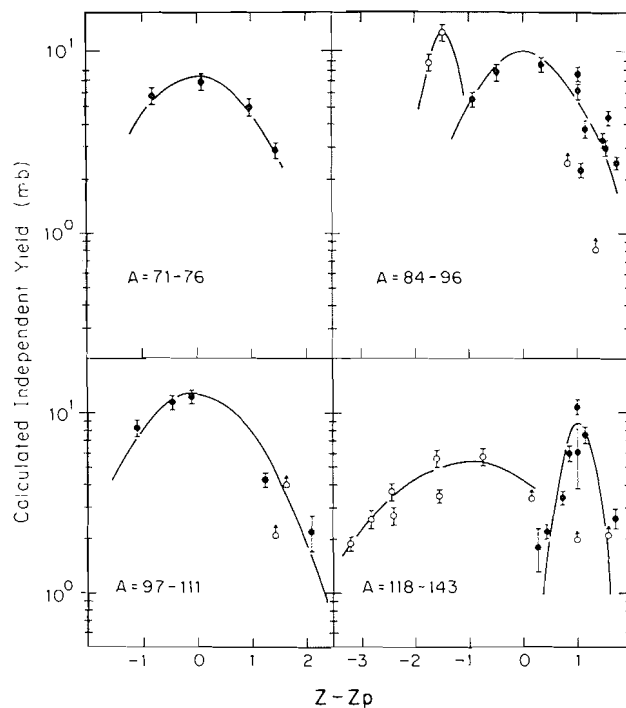


FIG. 3. The charge dispersion curves obtained in this work for the intermediate mass fragments are shown as a function of the mass region of the products.

The results of these measurements for the interaction of 28 GeV protons with  $^{238}\text{U}$  are summarized in Table 1. Also tabulated in Table 1 for comparison with the present data are other measurements of the target fragment yields in the interaction of  $^{238}\text{U}$  with protons of energy 11.5–29 GeV. (At proton energies above 10 GeV, the target fragment yields are known to be essentially independent of proton energy (8, 18).)

No corrections were made for reactions induced by secondary particles because we have no experimental measurement of the magnitude of the effect for our bombardment. Based upon the known systematics of such corrections (3), we would expect this correction to be very small, given the thickness of our target, for the neutron-deficient nuclides on which this paper focuses and to be 10% for the neutron-rich nuclei.

The measured cumulative-yield production cross sections (which include contributions from nuclei produced by radioactive decay) were corrected for this decay feeding by an iterative fitting of Gaussian distributions to the measured data in a manner described previously (19). These are shown in Table 1 as "calculated independent yield". In making this correction, one assumes Gaussian charge dispersions; i.e., the independent yield cross sections can be represented by a histogram that lies along a Gaussian curve, at constant mass number. This is written as:

$$[1] \quad \sigma(Z, A) = \sigma(A) \left\{ [2\pi s_z^2(A)]^{-1/2} \exp \left[ \frac{[Z - Z_p(A)]^2}{-2s_z^2(A)} \right] \right\}$$

with the three parameters:  $\sigma(A)$  the total isobaric yield,  $s_z(A)$  the Gaussian width parameter, and  $Z_p(A)$  the most probable  $Z$  value for that isobar. By assuming that  $\sigma(A)$  varies smoothly and slowly as a function of mass number  $A$  and is roughly constant within a small  $A$  range, one can iteratively fit the measured data, determining  $Z_p(A)$  and  $s_z(A)$  for limited mass regions. The results of this procedure are shown in Figs. 1, 2, and 3, with the values of  $s_z(A)$  and  $Z_p(A)$  being tabulated in Table 2. The values of  $s_z(A)$  are believed to be known to 0.1Z units while the values of  $Z_p(A)$  are believed to be known to  $0.3s_z(A)$ . In the mass regions (84–96, 97–111, and 118–143) where fission is an important contributor to the product yields, the charge dispersions are either very broad or double-humped, a fact previously noted (3). The

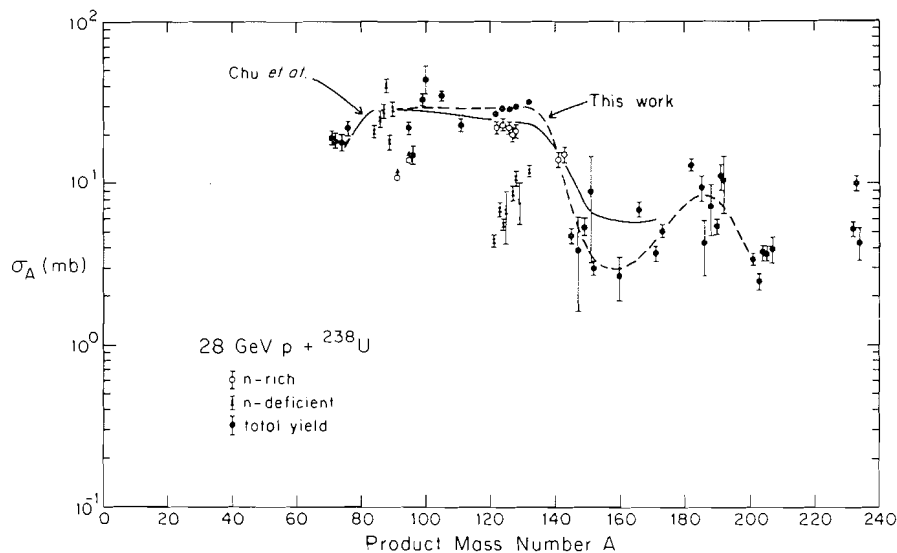


FIG. 4. The target fragment mass distribution,  $\sigma(A)$  obtained in this work for the interaction of 28 GeV protons with U is shown along with the previous radiochemical data (3). Closed circles represent the total isobaric yield while the open circles and crosses represent the isobaric yield of the n-rich and n-deficient species at a given A value. The dashed line is to guide the eye through the data of this work.

TABLE 2. Charge dispersion parameters<sup>a</sup>

Mass number range	$s_z$	$Z_p(A) = a + bA$	
		$a$	$b$
71-76	1.00	-0.380	0.450
84-96 neutron-rich	0.300	-1.69	0.439
84-96 neutron-deficient	0.900	-2.600	0.410
97-111	1.00	-1.00	0.439
118-143 neutron-rich	1.50	0.750	0.410
118-143 neutron-deficient	0.300	0.380	0.429
145-160	0.500	15.8	0.330
166-173	0.500	15.35	0.330
182-192	0.500	15.2	0.330
195-207	0.300	15.4	0.330
232-234	0.300	7.80	0.368

<sup>a</sup> $s_z(A)$  was taken to be roughly independent of A over a small A range and  $Z_p(A)$  was represented by a linear function of A over the same range.

isobaric or mass yield for each data point was calculated (19) and the resulting fragment mass distribution is shown in Fig. 4 and Table 1 along with the previously published work of Chu *et al.* (3).

## Results and discussion

### Heavy fragment yields

The primary focus of this paper is on the yields of the heavy ( $160 \leq A \leq 210$ ) fragments produced by the interaction of 28 GeV p with  $^{238}\text{U}$ . However, since the yields of many of these fragments were measured by off-line  $\gamma$ -ray spectroscopy of chemically separated fractions in which the chemical yields were determined by comparisons with the radionuclide activities in the unseparated foils, the accuracy of the heavy fragment measurements is directly related to the accuracy of all the radionuclide activity measurements. In Fig. 5, we compare the measured cumulative yield radionuclide production cross sections from this work with values determined previously for this or similar reactions (data from Table 1). The average ratio of the cross sections measured in this work to those determined previously is 1.10, indicating overall general agreement between this work and previous work. There is, however, a

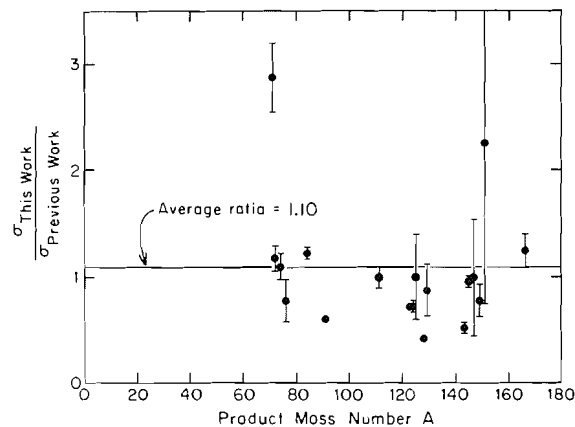


FIG. 5. The ratio of the measured nuclidic production cross sections in this work to those measured previously (see Table 1).

certain scatter to the ratios perhaps due to the fact that the values reported herein were the results of a single measurement rather than the combination of many measurements as frequently reported in the past.

The measured cumulative-yield radionuclide production cross sections for species with  $173 \leq A \leq 207$  range, in general, from 1 to 10 mb, indicating without a doubt that these fragments are produced in significant yields in the interaction of 28 GeV p with  $^{238}\text{U}$ . The charge dispersions for the species with  $182 \leq A \leq 207$  are moderately well-defined (Fig. 1) and thus the isobaric yields derived from them (Fig. 4) of 5-10 mb for these fragments appear to be reasonably well established (they do significantly exceed the measured radionuclide production cross sections because of the correction for unobserved members of the mass chains). The production of these heavy fragments is, therefore, a process with a total cross section of  $\sim 250$  mb. In any case, the yields of these fragments are significantly higher than would be expected for fission fragments based upon the shapes of the single fragment mass spectra (3, 13, 14), which show a pattern of sharply decreasing yields from  $A = 120$  to  $A = 170$  (where the isobaric yields are  $\sim 5$  mb).

Given the existence of significant yields of fragments with

$160 \leq A \leq 210$ , the question arises as to the mechanism for their formation. High energy proton induced reactions have generally been described in the framework of a two-step model in which the reaction proceeds via a first step of a fast intranuclear cascade as the incident proton interacts with the target nucleons followed by a slower second step in which the target residue of the first step deexcites by emission of nucleons or light nuclei or fission. Conventional intranuclear cascade calculations (20–22) of the first step of the reaction have been restricted to projectile energies of  $\sim 1000$  MeV/u where only single isobar or pion production is considered. Other calculational models for the first step of the reaction, such as the abrasion–ablation (23) or firestreak models (24, 25), which do work properly at projectile energies above 1000 MeV/u are not appropriate for proton-induced reactions. (In the firestreak model the incident proton is divided into collinear tubes leading to the stopping of pieces of the proton in the target, an unrealistic situation, while the abrasion–ablation model is generally thought (24) to treat the excitation energy given to the target residue in an overly simplistic and erroneous manner.) Thus we do not have a realistic calculational model for treating the first step of the reaction between a 28 GeV proton and a  $^{238}\text{U}$  nucleus.

Nonetheless we have attempted to pursue the question of the origin of the heavy ( $160 \leq A \leq 210$ ) fragments in a didactic manner. We have assumed an initial distribution of target fragment mass, charge, and excitation energy as might be appropriate for the first, fast stage of the p–U collision and then attempted to compute the final product distribution after deexcitation of these primary residues. In doing so, we can show the types of events that could lead to products in the  $160 \leq A \leq 210$  region. Figure 6 shows the shape of the assumed fragment distribution from the 28 GeV p +  $^{238}\text{U}$  reaction after the first, fast step of the reaction. (This distribution is predicted by the firestreak model (25) for the 28 GeV p +  $^{238}\text{U}$  reaction; a very similar distribution is predicted by the VEGAS intranuclear cascade code (20) for the interaction of 1 GeV protons with  $^{238}\text{U}$ .) The charge distributions associated with the  $A$  and  $E^*$  distributions of Fig. 6 are generally centered about the valley of  $\beta$ -stability.

The deexcitation of the members of this initial fragment distribution was calculated using the EVA3 code of McGaughey and Morrissey (26). EVA3 is a modification of the original stepwise Monte Carlo treatment (27–29) of the deexcitation of nuclei by particle emission and fission known as the DFF code. The original DFF code was modified to include a more realistic treatment of fission competition. The excitation energy ( $E^*$ ) dependence of  $\Gamma_f/\Gamma_n$  is given by (30)

$$[2] \quad \Gamma_f/\Gamma_n = \frac{4A^{2/3}a_f(E^* - B_n)}{[K_0a_n2a_f^{1/2}(E^* - E_f)^{1/2} - 1]} \times \exp[2a_n^{1/2}(E^* - B_n) - 2a_f^{1/2}(E^* - E_f)^{1/2}]$$

where  $\Gamma_f$  and  $\Gamma_n$  are the fission and neutron emission widths, respectively,  $A$  the mass number of the nucleus with excitation energy  $E^*$ , neutron binding energy  $B_n$ , fission barrier height  $E_f$ , and  $K_0$  is the rms value of the projection of the angular momentum on the nuclear axis of symmetry. The values of the level density parameters at the fission saddle point  $a_f$ , and the equilibrium deformation  $a_n$ , were chosen in a manner discussed later. The fission barrier heights are calculated using the simple approximate formula of Cohen and Swiatecki (31)

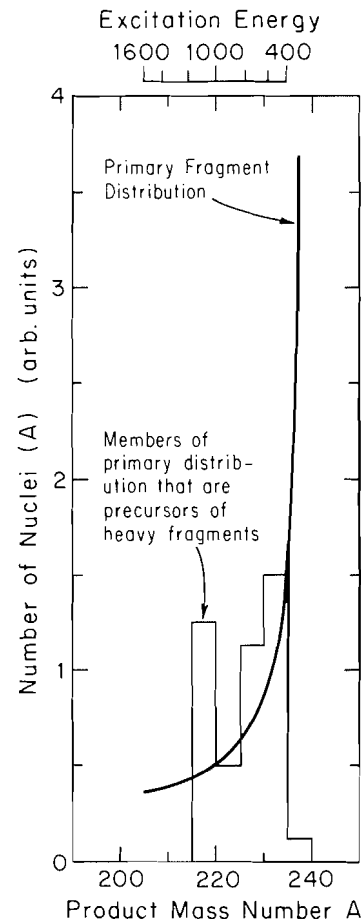


FIG. 6. The shape of the initial primary fragment distribution as a function of product mass number after the fast step of the reaction of 28 GeV p +  $^{238}\text{U}$ . Also shown are those members of the initial distribution which deexcited to produce final fragments with  $160 \leq A \leq 210$ .

$$[3] \quad \begin{aligned} E_f &= 0.38(0.75 - x)E_s^0 && \text{for } 1/3 \leq x \leq 2/3 \\ E_f &= 0.83(1 - x)^3E_s^0 && \text{for } 2/3 \leq x \leq 1 \end{aligned}$$

where the fissionability parameter,  $x$ , is given by

$$[4] \quad x = \frac{Z^2}{50.88A \left(1 - 1.7826 \left(\frac{A - 2Z}{A}\right)^2\right)}$$

and  $E_s^0 = 17.80A^{2/3}$ . The variations of the widths of the fission mass distributions as a function of the  $Z$ ,  $A$ , and  $E^*$  of the fissioning system are calculated using the formalism of Nix (32).

Several thousand deexcitation chains were followed to determine which members of the initial fragment distributions, if any, survive to form fragments with final mass numbers of  $160 \leq A \leq 210$ . The fraction of the initial population that survives to form heavy fragments is a very sensitive function of the level density parameters  $a_f$  and  $a_n$ . In Fig. 7 we show the results of two calculations of the final fragment distributions (starting with the initial fragment distribution of Fig. 6) made with two separate assumptions about  $a_f/a_n$ , i.e.,  $a_f/a_n = 1.0$  and  $a_f/a_n = 1.1$ . (Both of these choices for  $a_f/a_n$  are reasonable for the nuclei and excitation energies encountered (30).) The yields of the heavy fragments change dramatically with this small variation in  $a_f/a_n$ , as is illustrated in Fig. 7 and was also

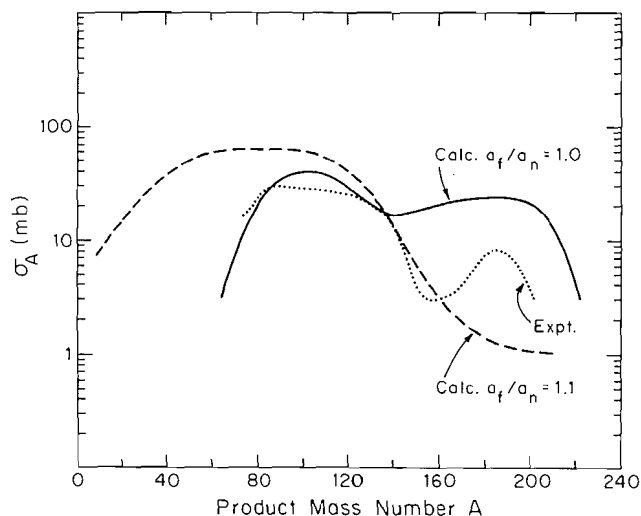


FIG. 7. The effect of two different values of  $a_f/a_n$  upon the calculated final fragment distribution is shown.

observed by Wilkins, Steinberg, and Kaufman (33). To study exactly which initial fragments survive fission decay to become heavy fragments, we arbitrarily fixed  $a_f/a_n$  using the formula

$$[5] \quad a_f = \left[ 1 + \frac{0.1}{\log_{10}(E^* - E_f)} \right] a_n$$

Using eq. [5] to fix the  $a_f/a_n$  ratio in our model, we then studied the outcome of  $\sim 3000$  deexcitation chains to see which members of the initial fragment population survived to become heavy fragments and how they "escaped" fission. In Fig. 6 we show those members of the initial fragment population that survived to form fragments with  $160 \leq A \leq 210$ . As one can see from examining Fig. 6, these survivors are fairly evenly distributed in mass number from 215 to 235. Because the initial distribution falls steeply with decreasing mass number, the lower mass initial fragments from the fast first stage of the reaction must have a greater probability of surviving to become heavy fragments despite their high excitation energy. This is, of course, due to the steeply decreasing fissionability of nuclei within the Ra-Th-U region with decreasing  $Z$  and  $A$ . Due to this, the yield of heavy fragments should increase in reactions with heavy targets where a larger fraction of the initial fragment distribution has lower  $Z$  and  $A$ . Thus greater heavy fragment yields are expected in the reaction of high energy protons with  $^{232}\text{Th}$  or in the reaction of relativistic heavy ions (which remove more mass from the target than protons) with  $^{238}\text{U}$ .

Deexcitation chains that lead to heavy fragments generally start, especially for primary fragments of high  $Z$  and  $A$ , with copious charged particle emission (to escape the region of high fissionability) followed by long chains of successive neutron emission (as the nuclei are very  $n$ -rich due to the charged particle emission). The average deexcitation chain leading from the primary to the final heavy fragment distribution removes 53 nucleons and approximately 770 MeV of excitation energy. The average number of particles emitted is 34, with the relative abundances:  $n$ -66%,  $p$ -9%,  $d$ -9%,  $t$ -9%,  $^3\text{He}$ -1%, and  $^4\text{He}$ -6%. The relative numbers of particles emitted are approximately what one would expect (27) for any heavy nucleus excited to 700 MeV. One might conclude that events producing fragments with  $160 \leq A \leq 210$  contain an unusually large fraction of the "deeper" spallation events from the fast initial

stage of the reaction, and of these events the ones leading to heavy fragment survivors consist of those which happen to begin their deexcitation by emitting several charged particles rather than fissioning.

#### Fission fragment yields

The most important new data reported in this paper are the yields of the heavy fragments from the interaction of 28 GeV protons with  $^{238}\text{U}$ . However, as remarked upon earlier, we did measure the yields of the fission fragments simultaneously with the heavy fragments and the two measurements are connected in a variety of ways. Figure 4 shows the isobaric yields of all the fragments (from the 28 GeV  $p + ^{238}\text{U}$  reaction) measured in this work along with a summary (3) of previous radiochemical measurements for this reaction. For the fragments with  $70 \leq A \leq 140$ , there is general agreement between the previous work and the isobaric yields from the current work (especially considering that the data reported herein are the result of a single measurement). The fragment yield distribution in this  $A$  region appears to have a plateau-like structure unlike the more sharply peaked fragment distribution seen (13, 34) in the reaction of 11.5 GeV protons with  $^{238}\text{U}$ . Some fragments with  $A < 70$  were observed as well, however the quality of the data was not as high as for the heavier fragments, so these data are not included.

In the fragment mass region  $140 \leq A \leq 160$ , there is general agreement between the *measured* cumulative yield cross sections of this work and previous work (Table 1, Fig. 5) but disagreement exists as to the isobaric yields that should be deduced from the measured data. The charge dispersions fitted to the data in this work are not well-defined because of the lack of measurements of *very* neutron-deficient and any possible neutron-rich species. In previous work (3), the charge distribution for  $A = 147$  was found to be double humped with significant neutron-deficient and neutron-rich components. The neutron-rich nuclides seen by Chu *et al.* (3) were not seen in this work and thus we have no evidence for a broad double-humped charge dispersion in this work. Therefore we conclude that any discrepancies between the isobaric yields measured in this work and previous work are more apparent than real. These discrepancies serve as a warning about the difficulty of deducing fragment isobaric yields in a complex reaction without an extensive set of primary measured radionuclide yields.

#### Conclusion

The principal things we have learned from this study are:

- (1) Heavy fragments ( $160 \leq A \leq 210$ ) are produced with significant yields in the interaction of 28 GeV protons with  $^{238}\text{U}$ .
- (2) These heavy fragments could result from primary fragments that have emitted large numbers of charged particles early in their deexcitation and could represent the "deeper" spallation portions of the primary fragment distribution.
- (3) We would expect larger production cross sections of heavy residues for proton induced reactions with lighter targets such as  $^{232}\text{Th}$  or  $^{208}\text{Pb}$ , or for heavy-ion induced reactions with  $^{238}\text{U}$ .

#### Acknowledgements

We wish to thank Marilyn Rodder for her help in performing the chemical separations and Dr. J. B. Cumming for arranging the AGS irradiation and the shipment of the sample to LBL.

This work was supported by the Director, Office of Energy

Research, Division of Nuclear Physics of the Office of High Energy and Nuclear Physics of the U.S. Department of Energy under Contract DE-AC03-76SF00098.

1. W. LOVELAND, R. J. OTTO, D. J. MORRISSEY, and G. T. SEABORG. *Phys. Rev. Lett.* **39**, 320 (1977).
2. P. L. MCGAUGHEY, D. J. MORRISSEY, W. LOVELAND, and G. T. SEABORG. Lawrence Berkeley Laboratory Report No. LBL-9711. 1980. p. 92.
3. Y. Y. CHU, E. M. FRANZ, G. FRIEDLANDER, and P. J. KAROL. *Phys. Rev.* **C4**, 2202 (1971).
4. J. B. CUMMING, G. FRIEDLANDER, J. HUDIS, and A. M. POSKANZER. *Phys. Rev.* **127**, 950 (1962); J. B. CUMMING. Private communication.
5. R. BRANDT. *Radiochim. Acta*, **16**, 148 (1972).
6. S. K. CHANG and N. SUGARMAN. *Phys. Rev.* **C8**, 775 (1973).
7. K. BEG and N. T. PORILE. *Phys. Rev.* **C3**, 1631 (1971).
8. O. SCHEIDEMANN and N. T. PORILE. *Phys. Rev.* **C14**, 1534 (1976).
9. J. A. PANONTIN and N. T. PORILE. *J. Inorg. Nucl. Chem.* **3**, 1775 (1970).
10. M. LAGARDE-SIMONOFF and G. N. SIMONOFF. *Phys. Rev.* **C20**, 1498 (1979).
11. Y. W. YU and N. T. PORILE. *Phys. Rev.* **C7**, 1597 (1973).
12. J. B. CUMMING and K. BACHMANN. *Phys. Rev.* **C6**, 1362 (1972).
13. B. D. WILKINS, E. P. STEINBERG, and S. B. KAUFMAN. *Phys. Rev.* **C19**, 856 (1979).
14. L. P. REMSBERG, F. PLASIL, J. B. CUMMING, and M. L. PERLMAN. *Phys. Rev.* **187**, 1597 (1969).
15. Y. W. YU, N. T. PORILE, R. WARASILA, and O. A. SCHAEFFER. *Phys. Rev.* **C8**, 1091 (1973).
16. J. V. KRATZ, J. O. LILJENZIN, and G. T. SEABORG. *Inorg. Nucl. Chem. Lett.* **10**, 951 (1974).
17. D. J. MORRISSEY, D. LEE, R. J. OTTO, and G. T. SEABORG. *Nucl. Inst. Meth.* **158**, 499 (1979).
18. P. M. STARZYK and N. SUGARMAN. *Phys. Rev.* **C8**, 1448 (1973).
19. D. J. MORRISSEY, W. LOVELAND, M. DE SAINT-SIMON, and G. T. SEABORG. *Phys. Rev.* **C21**, 1783 (1980).
20. K. CHEN, Z. FRAENKEL, G. FRIEDLANDER, J. R. GROVER, J. M. MILLER, and Y. SHIMAMOTO. *Phys. Rev.* **166**, 949 (1969).
21. G. D. HARP. *Phys. Rev.* **C10**, 2387 (1974).
22. H. W. BERTINI, A. H. CULKOWSKI, O. W. HERMANN, N. B. GOVE, and M. P. GUTHRIE. *Phys. Rev.* **C17**, 1382 (1978).
23. J. D. BOWMAN, W. J. SWIATECKI, and C. F. TSANG. Lawrence Berkeley Laboratory Report No. LBL-2908, 1973; D. J. MORRISSEY, W. R. MARSH, R. J. OTTO, W. LOVELAND, and G. T. SEABORG. *Phys. Rev.* **C18**, 1267 (1978).
24. W. D. MYERS. *Nucl. Phys.* **A296**, 117 (1978); J. GOSSETT, J. I. KAPUSTA, and G. D. WESTFALL. *Phys. Rev.* **C18**, 844 (1978).
25. P. L. MCGAUGHEY, D. J. MORRISSEY, and G. T. SEABORG. Lawrence Berkeley Laboratory Report No. LBL-11588, 1981. p. 159.
26. P. L. MCGAUGHEY and D. J. MORRISSEY. Private communication.
27. I. DOSTROVSKY, P. RABINOWITZ, and R. BIVINS. *Phys. Rev.* **111**, 1659 (1958).
28. I. DOSTROVSKY, Z. FRAENKEL, and P. RABINOWITZ. *Proc. 2nd UN Int'l Conf. Peaceful Uses of At. Energy* **15**, 301 (1958).
29. I. DOSTROVSKY, Z. FRAENKEL, and G. FRIEDLANDER. *Phys. Rev.* **116**, 683 (1959).
30. R. VANDENBOSCH and J. R. HUIZENGA. *Nuclear fission*. Academic, New York. 1973. p. 233.
31. S. COHEN and W. J. SWIATECKI. *Ann. Phys. NY*, **22**, 406 (1963).
32. J. R. NIX. *Nucl. Phys.* **A130**, 241 (1969).
33. B. D. WILKINS, E. P. STEINBERG, and S. B. KAUFMAN. *Phys. Rev.* **C19**, 856 (1979).
34. Y. W. YU. *Phys. Rev.* **C22**, 933 (1980).
35. G. FRIEDLANDER. *Physics and chemistry of fission*. Vol. II. 1965. p. 265.
36. J. HUDIS, T. KIRSTEN, R. W. STOENNER, and O. A. SCHAEFFER. *Phys. Rev.* **C1**, 2019 (1970).
37. E. M. FRANZ and G. FRIEDLANDER. *Phys. Rev.* **C4**, 1671 (1971).
38. K. BEG and N. T. PORILE. *Phys. Rev.* **C10**, 167 (1974).
39. N. T. PORILE. *Phys. Rev.* **148**, 1235 (1966).
40. Y. W. YU and N. T. PORILE. *Phys. Rev.* **C10**, 167 (1974).
41. Y. Y. CHU, E. M. FRANZ, and G. FRIEDLANDER. *Nucl. Phys.* **B40**, 428 (1972).
42. K. BACHMANN. *J. Inorg. Nucl. Chem.* **32**, 1 (1970).

**This article has been cited by:**

1. W. Loveland, A. M. Vinodkumar, D. Peterson, J. P. Greene. 2011. Synthesis of heavy nuclei using damped collisions: A test. *Physical Review C* **83**:4. . [[CrossRef](#)]
2. R. Yanez, W. Loveland, K. Aleklett, A. Srivastava, J. O. Liljezén. 1995. Heavy-residue production in Ar-Th collisions at 44, 77, and 95 MeV/nucleon. *Physical Review C* **52**:1, 203-218. [[CrossRef](#)]
3. B. Singh, J.A. Szucs. 1990. Nuclear data sheets for A = 100. *Nuclear Data Sheets* **60**:1, 1-137. [[CrossRef](#)]
4. Ben-Hao Sa, Yu-Ming Zheng, Xiao-Ze Zhang. 1990. Dependence of the phase transition on the mass number of hot nuclei before break-up. *Nuclear Physics A* **509**:3, 499-508. [[CrossRef](#)]
5. Zhang Dong, SA Ben-hao, Xiao-ze Zhang, Jin Xing Nan. 1989. A simplified method of the Monte Carlo simulation for the disassembly of hot nuclei. *Nuclear Physics A* **499**:3, 487-494. [[CrossRef](#)]
6. B. Singh, D.A. Viggars. 1987. Nuclear data sheets for A = 74. *Nuclear Data Sheets* **51**:2, 225-327. [[CrossRef](#)]
7. Xiao-Ze Zhang, D.H.E. Gross, Shu-Yan Xu, Yu-Ming Zheng. 1987. On the decay of very hot nuclei (I). Canonical metropolis sampling of multifragmentation. *Nuclear Physics A* **461**:3-4, 641-667. [[CrossRef](#)]
8. Xiao-Ze Zhang, D.H.E. Gross, Shu-Yan Xu, Yu-Ming Zheng. 1987. On the decay of very hot nuclei (II). Microcanonical metropolis sampling of multifragmentation. *Nuclear Physics A* **461**:3-4, 668-690. [[CrossRef](#)]
9. D.H.E. Gross, Xiao-ze Zhang. 1985. Fragmentation of big nuclei by protons at high energies - Monte Carlo sampling of the open phase-space. *Physics Letters B* **161**:1-3, 47-51. [[CrossRef](#)]
10. J. Hüfner. 1985. Heavy fragments produced in proton-nucleus and nucleus-nucleus collisions at relativistic energies. *Physics Reports* **125**:4, 129-185. [[CrossRef](#)]
11. Sa Ban-Hao, D.H.E. Gross. 1985. Finite-size effects and statistical approach to nuclear fragmentation processes: Monte Carlo simulation. *Nuclear Physics A* **437**:3-4, 643-668. [[CrossRef](#)]
12. P. L. McGaughey, W. Loveland, D. J. Morrissey, K. Aleklett, G. T. Seaborg. 1985. Uranium target fragmentation by intermediate and high energy C 12 and Ne 20 ions. *Physical Review C* **31**:3, 896-909. [[CrossRef](#)]
13. B. Singh, D.A. Viggars. 1984. Nuclear Data Sheets for A=76. *Nuclear Data Sheets* **42**:3, 233-368. [[CrossRef](#)]